Twenty-first Symposium (International) on Combustion/The Combustion Institute, 1986/pp. 521–529

EXPLOSIONS OF ADIABATICALLY COMPRESSED GASES IN A CONSTANT VOLUME BOMB

JAMES C. KECK AND HAORAN HU
Massachusetts Institute of Technology
Cambridge, Massachusetts 02139

Measurements of the explosion limits for fuel-air mixtures compressed by an expanding laminar flame front have been made in a constant volume bomb. The mixtures studied to date include normal pentane, hexane and heptane with fuel-air equivalence ratios in the range 0.8 to 1.3. An Arrhenius plot of the explosion density as a function of reciprocal temperature in the range 670 to 720 K is consistent with an activation energy of 51 kcal/mole. For fixed initial temperature and pressure the explosion density has a weak minimum at an equivalence ratio near $\phi = 1.1$ and decreases with increasing chain length. This behavior is in good agreement with observations made in rapid compression machines and spark ignition engines.

A simple kinetic model based on a branched chain mechanism has been developed to correlate the data. In the first stage region the equations are linear and can be integrated approximately using the WKB method. The resulting expression gives an explicit connection between the explosion limit for gases undergoing adiabatic compression and the first stage induction time at constant density. Quantitative agreement between theory and experiment can be achieved with minor modifications in values of published rate constants.

I Introduction

The explosion of adiabatically compressed combustible gas mixtures is one of the simplest and most important combustion processes and determining the mechanism involved has been a major goal of combustion research for the past half century.

Although the mechanism of hydrogen oxidation is relatively well understood[1,2] and encouraging progress is currently being made on the modeling of laminar flames for simple hydrocarbons[3,4], our present understanding of the rapid oxidation of higher hydrocarbons is relatively poor. Experimental results obtained in closed vessels[5], fast mixing reactors[6], rapid compressing machines[7–9], and reciprocating piston engines[10–12] have not yet been satisfactorily correlated and data obtained in rapid compression machines operating under similar conditions disagree[7,8]. In addition kinetic models used by different authors vary considerably[13–18] and the rate constants for hydrocarbons with more than one carbon atom are based largely on estimates[16,17,25]. Thus there is a need for further experimental studies carried out under controlled conditions as well as further kinetic modeling.

II Experimental Procedure and Results

The combustion bomb used in the present experiments is shown schematically in Fig. 1 and a description of the complete facility and operating procedure can be found in reference 20. The bomb has an inner diameter of 15.24 cm and is designed to operate at initial temperatures up to 500 K and final pressures up to 10.1 mPa. The initial gas mixture is prepared in the bomb using the method of partial pressures by admitting first the fuel and then the air. A settling time of approximately 5 minutes is allowed for the mixture to come to thermal equilibrium with the walls and the turbulence produced by the inlet jet to decay. The mixture is then ignited at the center by a spark between two extended radial electrodes. This produces a spherical laminar flame which expands radially compressing the unburned gas ahead of it in a manner similar to that in which the turbulent flame compresses the unburned charge in a spark-ignition engine.

At low initial temperatures and pressures, the gas mixture burns smoothly to completion as shown by the pressure vs. time trace in the upper oscillogram in Fig 2. This oscillogram also shows three ionization probe traces used to check the spherical symmetry of the flame by measuring its arrival times at several locations on the bomb wall.

At high initial pressures, the situation is markedly different and an abrupt increase in pressure followed by large oscillations occurs prior to completion of burning as shown in the two lower oscillograms in Fig. 2. These pressure

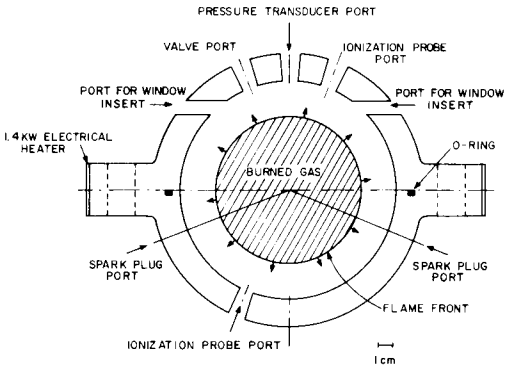

FIG. 1. Schematic diagram of the constant volume spherical combustion bomb used to determine explosion limits.

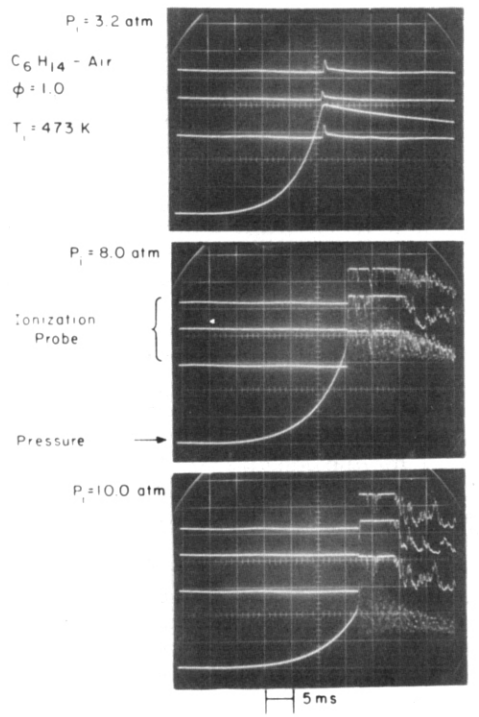

FIG. 2. Oscillograph records showing pressure and ionization current traces for various initial pressures. The upper record is typical of normal burning; the two lower records are typical of cases in which an explosion of the end gas occurs prior to completion of normal burning.

traces are virtually identical to those observed for rapid compression machines[7], and spark-ignition engines operating under "knocking" conditions[21]. At the time of the abrupt pressure increase large signals are observed on all ionization probes traces. The dispersion in these signals is less than 50 μs suggesting that the explosion of the remaining unburned charge is effectively homogeneous.

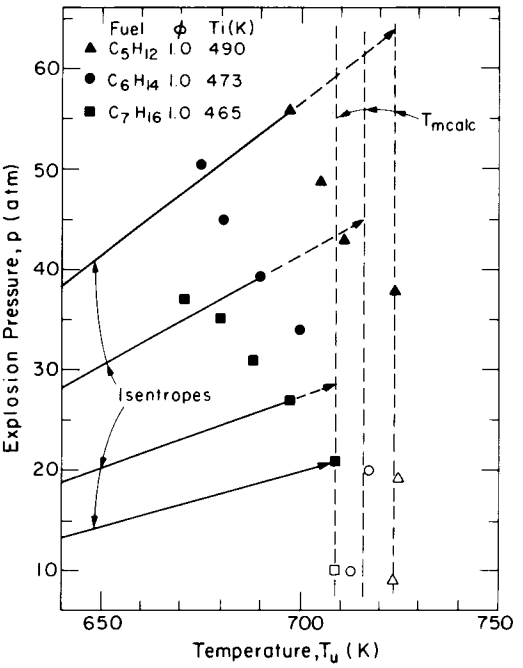

FIG. 3. Explosion pressures as a function of unburned gas temperatures for n-pentane, n-hexane and n-heptane. Open symbols represent cases in which the charge burned to completion without an end gas explosion. Vertical dashed lines show maximum temperature reached if no explosion occurs.

An example of the explosion limits observed in the constant volume bomb for several normal alkane fuels is shown by the plots in Fig. 3. The solid symbols indicate the pressure and unburned gas temperature at which the explosion occurred. The diagonal solid lines show the isentropes along which the unburned core gas outside the thermal boundary layers is compressed, and the open symbols and vertical dashed lines show the final temperature for the case where the gas mixture burns smoothly to completion. The magnitude of the observed explosion pressure as well as its dependence on temperature and molecular weight are all in good agreement with observations made in rapid compression machines and spark-ignition engines.

III Reduced Kinetic Model

The elementary reactions involved in the oxidation of hydrocarbons have been the subject of numerous investigations over the past fifty

years and many kinetic models for describing the homogeneous explosion of hydrocarbon-oxygen-diluent mixtures have developed. Excellent reviews of this work can be found in references 2,16,22. In general it is agreed that the oxidation process involves a complex branched chain mechanism which leads to a 2-stage ignition characterized by an an initial delay interval of duration t_I during which the radical concentration rises exponentially but the sensible energy release is negligible, followed by a second interval of duration t_{II} during which the reactions go to completion and the temperature rises to its final value often in a series of steps.

Although there is little doubt that the analysis of the second stage involves a large number of reaction equations requiring numerical integration, it seems probable that the first stage can be treated using a carefully selected "reduced" set of reaction equations which can be integrated analytically. Such a "reduced kinetic model" based largely on suggestions by Benson[16] is shown schematically in Fig. 4. It is expected to be valid for normal alkanes with carbon numbers greater than 4 at low temperatures, $T <$ 800 K, and high oxygen concentrations, $[O_2] > V_o^{-1}$, where $V_o = 22{,}400$ cc is the standard molar volume.

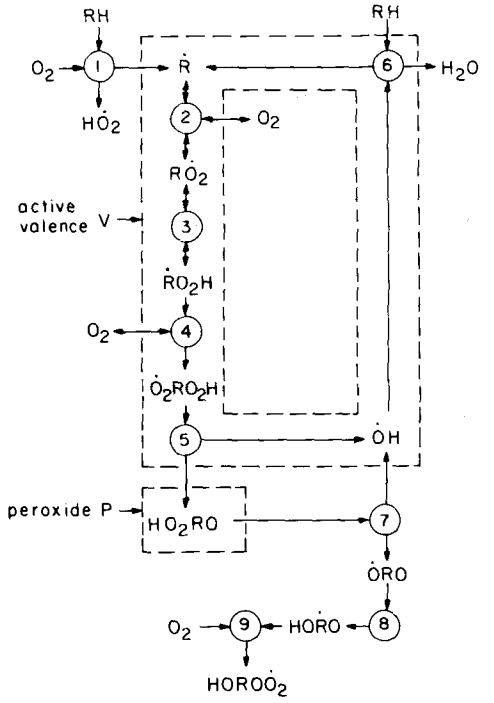

FIG. 4. Branched chain model for high pressure, low temperature explosions.

Oxidation is assumed to be initiated by the hydrogen abstraction reaction:

$$RH + O_2 \rightarrow \dot{R} + H\dot{O}_2 \qquad (R1)$$

where $\dot{R}$ is a normal alkane radical. The main chain involves the sequence of reactions:

$$\dot{R} + O_2 \longleftrightarrow R\dot{O}_2 \qquad (R2)$$
$$R\dot{O}_2 \longleftrightarrow \dot{R}O_2H \qquad (R3)$$
$$\dot{R}O_2H + O_2 \rightarrow \dot{O}_2RO_2H \qquad (R4)$$
$$\dot{O}_2RO_2H \rightarrow \dot{O}H + HO_2RO \qquad (R5)$$
$$\dot{O}H + RH \rightarrow \dot{R} + H_2O. \qquad (R6)$$

Branching occurs as a result of the reactions:

$$HO_2RO \rightarrow \dot{O}H + \dot{O}RO \qquad (R7)$$
$$\dot{O}RO \rightarrow HOR\dot{O} \qquad (R8)$$
$$HOR\dot{O} + O_2 \rightarrow HOROO_2. \qquad (R9)$$

In the prethermal stage, the forward rates of R2–R6 are large compared to the forward rates of R1 and R7 while the reverse rates of R1 and R4–R9 are negligible. Under these conditions, the chain R2–R6 is amenable to steady state analysis and the chain propagation rate is given by

$$k_c V = R_2^+ - R_2^- = R_3^+ - R_3^- = R_4^+ = P_\pm^+ = R_6^+, \qquad (1)$$

where k_c is the chain propagation rate constant,

$$V = \dot{R} + R\dot{O}_2 + \dot{R}O_2H + \dot{O}_2RO_2H + \dot{O}H \qquad (2)$$

is the active valence and the forward and reverse reaction rates are given by

$$R_2^+ = k_2^+[O_2]\dot{R} = \dot{R}/\tau_2^+ \qquad (3a)$$
$$R_2^- = k_2^- R\dot{O}_2 = R\dot{O}_2/\tau_2^- \qquad (3b)$$
$$R_3^+ = k_3^+ R\dot{O}_2 = R\dot{O}_2/\tau_3^+ \qquad (3c)$$
$$R_3^- = k_3^- \dot{R}O_2H = \dot{R}O_2H/\tau_3^- \qquad (3d)$$
$$R_4^+ = k_4^+[O_2]\dot{R}O_2H = \dot{R}O_2H/\tau_4^+ \qquad (3e)$$
$$R_5^+ = k_5^+ \dot{O}_2RO_2H = \dot{O}_2RO_2H/\tau_5^+ \qquad (3f)$$
$$R_6^+ = k_6^+[RH]\dot{O}H = \dot{O}H/\tau_6^+ \qquad (3g)$$

In Eqs (3a–3g) k_i^+ and k_i^- are the forward and reverse rate constants for reaction i and τ_i^+ and τ_i^- are the corresponding characteristic reaction times. Note that the radical $HOR\dot{O}O_2$ produced by the sequence R7–R9 has been assumed to be effectively inactive.

TABLE 1

(a) Arrhenius parameters for the equilibrium constant $K = Ae^{-E/RT}$ and rate constants $k^{\pm} = A^{\pm}e^{-E^{\pm}/RT}$. Units: moles, cc, s, kcal

Reaction	$\Delta H_{300}°$	log A	E	log A^+	E^+	log A^-	E^-	Refs
1 $RH + O_2 \rightarrow \dot{R} + H\dot{O}_2$	46.4	1.5	46	13.5	46	12.0	0	16
2 $\dot{R} + O_2 \rightarrow R\dot{O}_2$	− 31.0	− 1.4	− 27.4	12.0	0	13.4	27.4	16,24
3 $R\dot{O}_2 \rightarrow \dot{R}O_2H$	7.5	0.9	8.0	11.9	19	11.0	11	25
4 $\dot{R}O_2H + O_2 \rightarrow \dot{O}_2RO_2H$	− 31	− 1.9	− 27.4	11.5	0	13.4	27.4	
5 $\dot{O}_2RO_2H \rightarrow \dot{O}H + HO_2RO$	− 26.6			11.3	17			25
6 $\dot{O}H + RH \rightarrow \dot{R} + H_2O$	− 23.5			13.3	3			26
7 $HO_2RO \rightarrow H\dot{O} + \dot{O}RO$	43.6			15.6	43			16,27
8 $\dot{O}RO \rightarrow H\dot{O}RO$	− 8.5			11.0	10			16
9 $H\dot{O}RO + O_2 \rightarrow HORO\dot{O}_2$	− 31	− 1.9	− 27.4	11.5	0	13.4	27.4	
10 $\dot{R} + O_2 \rightarrow H\dot{O}_2 + C = C$	−13.5	0	− 13.5	11.5	6	11.5	19.5	16
11 $HO_2 + RH \rightarrow \dot{R} + H_2O_2$	8.0	0.9	8.0	11.7	16	10.8	8	16
12 $H_2O_2 + M \rightarrow 2\dot{O}H + M$	51.4	0.8	50.0	17.1	46	16.3	−4	28
13 $R\dot{O}_2 + RH \rightarrow \dot{R} + RO_2H$	8.0	1.1	8.0	11.2	16	10.1	8	16
14 $\dot{R}O_2H \rightarrow \dot{O}H + R'O + C = C$				14.4	31			17

(b) Comparison of calculated and measured rate parameters.

Fuel	E_o	log A_o	log A_{om}	log A_{3m}
C_5H_{12}	25.5	10.7	10.4	0.3
C_6H_{14}	25.5	10.7	10.5	0.5
C_7H_{16}	25.5	10.7	10.7	0.9

Combining Eqs. (1) and (3a–3g) gives the steady state radical concentrations:

$$\dot{O}H = V\, k_c \tau_6^{+} \tag{4a}$$

$$\dot{O}_2RO_2H = V\, k_c \tau_5^{+} \tag{4b}$$

$$\dot{R}O_2H = V\, k_c \tau_4^{+} \tag{4c}$$

$$R\dot{O}_2 = V\, k_c\, (\tau_3^{+} + \tau_4^{+}\tau_3^{+}/\tau_3^{+}) \tag{4d}$$

$$\dot{R} = V\, k_c(\tau_2^{+} + (\tau_3^{+} + \tau_4^{+}\tau_3^{+} / \tau_3^{-})\, \tau_2^{+}/\tau_2^{-}) \tag{4e}$$

and substitution of these expressions into Eq. (2) gives the characteristic cycle time

$$\tau_c = k_c^{-1} = \tau_6^{+} + \tau_5^{+} + \tau_4^{+} + \tau_3^{+}\,(1 + \tau_4^{+}/\tau_3^{+})\,(1 + \tau_2^{+}/\tau_2^{-}) + \tau_2^{+}. \tag{5}$$

The characteristic reaction times appearing in Eq. (5) have been calculated using the rate data summarized in Table 1a for conditions representative of those investigated in the constant volume bomb and rapid compression machines and are shown on the Arrhenius plot in Fig. 5. Also shown are the reaction times for several competing reactions, R10–R14, omitted from the present model. Although these reactions are expected to play an essential role in the analysis of 2-stage ignition at temperatures above 800 K[16,17], the curves in Fig. 5 indicate they are unimportant for the determination of the first stage induction time t_I at lower temperatures. In addition all radical-radical and radical-intermediate reactions have been omitted because the concentrations of radicals and intermediates in the prethermal stage is sufficiently low to make such reactions negligible.

It can be seen from Fig. 5 and Eq. (5) that for $T < 800$ K, $\tau_1^{+} \gg \tau_7^{+} \gg \tau_c$. Thus the use of the steady state approximation is well justified in this range and the rate equations for the active valance and the hydroperoxide can be written

$$\dot{V} = O_2/\tau_1^{+} + \Pi\Pi\tau_7^{+} \tag{6}$$

$$\dot{P} = V/\tau_c - P/\tau_7^{+} \tag{7}$$

where P = HO_2RO. The corresponding energy equation for an ideal gas undergoing adiabatic compression is

$$(C_p/R)\dot{T}/T = \dot{p}/p + \dot{Q}_r/MRT \tag{8}$$

where C_p is the constant pressure molar heat capacity, R is the universal gas constant, M is the number of moles of gas and

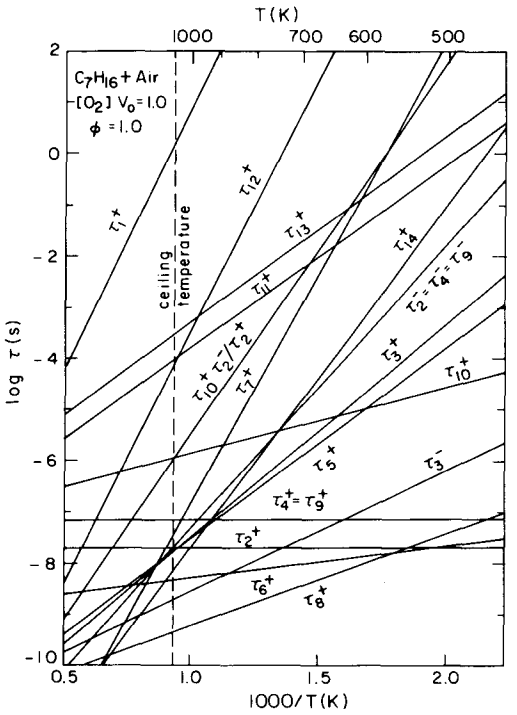

FIG. 5. Arrhenius plot of characteristic reaction times defined in the text calculated from data in Table 1a for representative conditions.

$$\dot{Q}_r = -\sum_i (R_i^+ - R_i^-)\Delta H_i \qquad (9)$$

is the rate of energy release due to chemical reactions. In Eq. (9), ΔH_i is the enthalpy the change in reaction i.

Using Eqs (1), (6) and (7) and the steady state assumption $R_9^+ = P_8^+ = P_7^+ = \Pi\Pi\tau_7^+$, Eq. (9) can be integrated to give

$$Q_r = Q_c P + (Q_c + Q_p)V, \qquad (10)$$

where

$$Q_c = -\sum_2^6 \Delta H_i = 107.5 \text{ kcal/mole} \qquad (11a)$$

$$Q_p = -\sum_7^9 \Delta H_i = -4.1 \text{ kcal/mole} \qquad (11b)$$

and the very small term O_2/τ_1^+ in Eq. (6) has been neglected. The fractional pressure rise in the gas due to chemical reactions can now be estimated from the relation

$$(\Delta p/p)_r \approx Q_r/MRT \qquad (12)$$

Assuming $T \approx 700$ K, $M/O_2 \approx 5$ and $V \ll P$, Eqs (11)–(13) give

$$(\Delta p/p)_r \approx 15\ (P/O_2) \qquad (13)$$

The first stage induction time t_I may be defined as the time when the pressure rise in the gas due to chemical reactions becomes measurable, This will occur when $(\Delta p/p)_r$ is of order one percent at which point P/O_2 will be of order 10^{-3}. Thus oxygen consumption is negligible and Eqs (6) and (7) are linear.

For a step rise in temperature such as that occurring behind a shock wave or approximated in a rapid compression machine or fast mixing process, Eqs (6) and (7) can be integrated to give

$$P/O_2 = (\tau_7^+/\tau_1^+)(\cosh \lambda\tau - 1) \qquad (14)$$

and

$$V/P = (\tau_c/\tau_7^+)^{1/2} \sinh \lambda t/(\cosh \lambda t - 1) \qquad (15)$$

where

$$\lambda = (\tau_7 + \tau_c)^{-1/2} \qquad (16)$$

and it has been assumed consistent with the use of the steady state approximation that $\tau_7^+ \gg \tau_c$. For $\lambda t \gg 1$, Eqs (14) and (15) reduce to

$$P/O_2 = (\tau_7^+/2\tau_1^+)e^{\lambda t} \qquad (14a)$$

$$V/P = (\tau_c/\tau_7^+)^{1/2} \qquad (15a)$$

For a slowly rising temperature such as that occurring in a constant volume bomb or spark ignition, Eqs (6) and (7) can be integrated approximately using the WKB method to obtain

$$P/O_2 = (\tau_7^+/2\tau_1^+)\ e^{\lambda\tau_\beta} \qquad (17)$$

$$V/P = (\tau_c/\tau_7^+)^{1/2}, \qquad (18)$$

where

$$\tau_\beta = \left(\frac{d \ln \lambda}{dt}\right)^{-1} = \left(\frac{2RT}{E_c + E_7}\right)\left(\frac{d \ln T}{dt}\right)^{-1} \qquad (19)$$

is a characteristic thermal rise time and E_c and E_7^+ are the activation energies for the rate constants k_c and k_7^+. The condition for the validity of Eqs (17) and (18) is $\lambda t > \lambda\tau_\beta > 1$. Note that Eqs (17) and (18) are identical to (14a) and (15b) except for the replacement of t by τ_β.

If it is now assumed in accord with the previous discussion of the energy equation, that thermal effects will be observable when P/O_2 rises above some critical value $(P/O_2)_I$, of order 10^{-3}, Eqs (14a) and (17) can be combined to give

$$t_I = \tau_\beta = (\tau_7^+\tau_c)^{1/2} \ln(2\tau_1^+/\tau_7^+)\ (P/O_2)_I \qquad (20)$$

stage induction time t_I observable in rapid compression machines and the thermal rise time τ_β at the explosion limit observable in the constant volume bomb.

At low temperatures where $\tau_3^- > \tau_4^+$, the dominant term in Eq. (5) for τ_c is τ_3^+ and Eq. (20) becomes

$$t_I = \tau_\beta = (k_7^+ k_3^+)^{-1/2}(12.3 - \ln[\mathrm{RH}]V_o) \quad (21)$$

in which rate constants have been substituted for characteristic times and the slowly varying logarithmic term has been evaluated using the Arrhenius parameters for k_1^+ and k_7^+ in Table 1a and nominal values of $(P/O_2)_I = 10^{-3}$ and T = 700 K. At higher temperatures where $\tau_3^- < \tau_2^+$the dominant term in Eq. (5) is $\tau_3^+\tau_4^+/\tau_3^- = (K_3 k_4^+[\mathrm{O_2}])^{-1}$, where K_3 is the equilbrium constant for Reaction R3, and Eq. (20) becomes

$$t_I = \tau_\beta = (k_7^+ K_3 k_4^+[\mathrm{O_2}])^{-1/2} (12.3 - \ln[\mathrm{RH}]V_o) \quad (22)$$

For $\tau_3^- > \tau_4^+$, Eq. (21) shows t_I and τ_β are independent of the oxygen concentration while for $\tau_3^- < \tau_4^+$, Eq. (22) shows that t_I and T_β are proportional to $[\mathrm{O_2}]^{-1/2}$. In both cases the dependence of t_I and τ_β on the fuel concentration is very weak.

For $p > 1$ mPa and temperatures in the range $650 < T < 800$ K, the present bomb experiments as well as previous experiments in rapid compression machines and spark ignition engines clearly show an important dependence of the explosion limit and first stage induction time on pressure. This indicates that under these conditions Eq. (22) is applicable and Reaction R4 rather than R3 is rate limiting. Estimates of the rate constant k_3^+ have been made by Baldwin et al.[24] while steric considerations suggest that k_4^+ should be somewhat smaller than k_2^+ for which Benson's estimate[16] has been used. As can be seen in Fig. 5, the requirement $\tau_3^- < \tau_4^+$ for T > 650 K can just be met if $k_4^+ \approx k_2^+/3$. In this connection it is interesting to note that in their analysis of 2-stage ignition in the Thornton rapid compression machine, Cox and Cole found it necessary to set $k_4^+ \approx k_2^+/200$ while at the same time increasing k_7^+ by a factor of 100 above the measured value[26].

IV Comparison of Experiment and Theory

To compare Eq. (22) with the currently available experimental data, it is convenient to use the Arrhenius form

$$\log [\mathrm{O_2}]V_o\tau_\beta^2 = -2(\log A_o - E_o/2.3\mathrm{RT}) \quad (23)$$

where

$$\log A_o = \tfrac{1}{2}\log A_3 A_4^+ A_7^+/V_o - \log(12.3 - 2.3\log[\mathrm{RH}]V_o \quad (24)$$

and

$$E_o = \tfrac{1}{2}(E_3 + E_4^+ + E_7^+) \quad (25)$$

Equation (23) shows that the explosion limit in a gas undergoing adiabatic compression depends not only on the temperature and density but also on the characteristic thermal rise time τ_β.

Equation (19) and data of the type shown in Fig. 3 have been used to calculate the values of $[\mathrm{O_2}]V_o\tau_\beta^2$ shown by the points on the Arrhenius plot in Fig. 6. The unburned gas temperatures T_u were calculated from the initial temperature T_i and the pressure ratio p/p_i assuming isentropic compression with variable γ_u. The largest source of error occurred in the pressure measurement and was due almost entirely to an estimated 3 percent accuracy with which the oscillograms could be read. The estimated error in $[\mathrm{O_2}]V_o\tau^2{}_\beta$ is the size of the points; the error in T_u is ±5 C and is shown by the representative horizontal error bars.

Also shown in Fig. 6 by the broken curves are values of $[\mathrm{O_2}]V_o t_I^2$ obtained from rapid com-

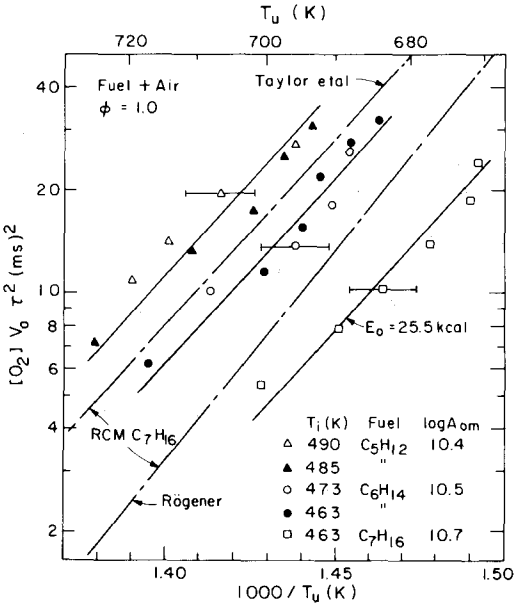

FIG. 6. Correlation of experimental data based on Eq. (23). The points show the results of this investigation. The solid lines are "best fits" to the points for a theoretical activation energy of 25.5 kcal. The broken lines are results from rapid compression machine experiments.

pression machine experiments[7,28]. Considering the sensitivity of the measurements to the absolute temperature determination the agreement both in the magnitude and the temperature dependence of the results is remarkably good and well within the combined uncertainties of the various measurements. An important conclusion which can be drawn from this comparison is that compression of the gas by a hot radical rich flame front rather than a cold solid piston has little effect on the explosion process.

Due to the extremely narrow temperature range covered by the data, the activation energy E_o is Eq. (23) is not well determined by the bomb measurements. We have therefore used Eq. (25) and the data in Table 1a to calculate the expected activation energy and used the data in Fig. 6 to determine the preexponential factors A_{om} for the three fuels studied. These values are given in Table 1b along with the corresponding calculated values of A_o. It can be seen that the measured values of A_{om} increase with increasing molecular weight and match the calculated value for heptane. This is consistent both with prior measurements and with the expected behavior of the equilibrium constant for reaction R3. The measured values A_{3m} are also given in Table 1b.

V Summary and Conclusions

1) Explosion limits measured in constant volume bombs and first stage induction times measured in rapid compression machines at temperature below 800 K and pressures above 1 mPa are essentially independent of fuel concentration and scale as $t_I[O_2]^{1/2}$.
2) A simple second order branched chain model can be used to fit data from both the constant volume bomb and rapid compression machines with relatively minor modifications in previously published rate constants.
3) Comparison of constant volume bomb and rapid compression machine results shows no significant different between compression by a hot flame front or a cold piston.
4) Ionization probe signals indicate that "explosion" of the gas in the constant volume bomb is effectively homogeneous.

Acknowledgement

This work was supported by a grant from the Department of Energy under contract number DE-AC04-81AL16310.

REFERENCES

1. Lewis, B. and von Elbe, G.: Combustion, Flames and Explosions of Gases, Academic Press, N.Y. 1951.
2. Dixon-Lewis, G. and Williams, D.J.: Comprehensive Chemical Kinetics, Vol 17, C.H. Bamford and C.F.H. Tipper, Eds., Elsevier, Amsterdam 1977
3. Westbrook, C. and Dryer, F., Combust. Flame, *37* 171 (1980).
4. Warnatz, J., 18th International Comb. Symp. 369 (1981).
5. Pollard, R.T.: Comprehensive Chemical Kinetics, Vol 17, C.H. Bamford and C.F.H. Tipper, Eds., Elsevier, Amsterdam (1977).
6. Dryer, F.L. and Brezinski K., Combust. Sci. and Tech. *45* 199 (1985).
7. Taylor, C.F., Taylor, E.S., Livingood, J.C., Russell, W.A. and Leary, W.A., SAE Transactions *4* 232 (1950).
8. Halstead, M.P., Kirsch, L.J. and Quinn, C.P., Combust. Flame *30* 45 (1977).
9. Griffiths, J.F. and Hasko, M.S., Proc. R. Soc. Lond. *A393* 371 (1984).
10. Taylor, C.F. and Taylor, E.S.: The Internal Combustion Engine, International Textbook Co., Scranton, PA 1966.
11. Obert, E.F., Internal Combustion Engines and Air Pollution, Intext Educational Publishers, New York, (1973).
12. Pahnke, A, Cohen, P. and Sturgis, B., Ind. Eng. Chem. *46* 1024 (1954), SAE Trans *63* 253 (1955).
13. Trumpy, D.K., Uyehara, O.A. and Myers, P.S., SAE Trans *78* 1849 (1969).
14. Livingood, J.C. and Wu, P.C., 5th International Combustion Symposium p. *34*, The Combustion Institute (1955).
15. Halstead, M.P., Kirsch, L.J., Prothero, A. and Quinn, C.P., Proc. R. Soc. Lond. A*346* 515 (1975).
16. Benson, S.W., Prog. Energy Combust. Sci. 7 125 (1981), see also Oxidation Communications *2* 169, (1982).
17. Cox, R.A. and Cole, J.A., Combust. Flame *60* 109 (1985).
18. Pitz, W.J. and Westbrook,, C.K., Combust. Flame *63* 113 (1986).
19. Benson, S.W., Thermochemical Kinetics, Wiley, (1976).
20. Metghalchi, M. and Keck, J.C., Combust. Flame *38*, 143 (1980).
21. Lightfoot, N.S. and Negus, C.R., 20th International Symposium on Combustion, p. 111, The Combustion Institute (1984).
22. Hucknall, D.J., Chemistry of Hydrocarbon Combustion, Chapman and Hall, London, (1985).
23. Morgan, C.A. Pilling, M.J. and Tullock, J.M., J. Chem. Soc., Faraday Trans. *II 78* 1323 (1982).

24. BALDWIN, R.R. HISKAM, M.W.M., WALKER, R.W., J. Chem. Soc., Faraday Trans. *178* 1615 (1982).
25. COHEN, N. AND WESTBURG, K.R., Aerospace Report No. ATR-82(7888)-3 (1982).
26. SAHETCHIAN, K.A., HEISS, A., RIGNY, R. AND BEN-AIM, R.I., Int. J. Chem. Kinet. *14* 1325 (1982).
27. BAULCH, D.L., DRYSDAL, D.D., DUXBURY, J. AND GRANT, S., Evaluated Kinetic Data for High Temperature Reactions, p.3 Butterworths, London, 1976.
28. ROGENER, H., Z. Elektrochem *53* 389 (1949).

COMMENTS

C. Morley, Shell Research. The mechanism used is suitable only for cool flames and cannot be used to predict a true ignition. How can you compare the results with experimental measurements on true ignition?

Author's Reply. It is known from experiments in rapid compression machines that for near stoichiometric mixtures at temperatures $T_u \lesssim 750°K$ and oxygen concentrations $[O_2]V_o \gtrsim 1$, the second stage induction duration is short compared to the first stage induction time. Thus, under these conditions only the so-called cool flame reactions are necessary to calculate total induction times and corresponding explosion limits. To extend the model to higher temperatures, it will obviously be necessary to include additional second stage reactions in the model and we are currently engaged in doing this.

●

C. Westbrook, Lawrence Livermore National Lab. Do you have plans to extend your approach to branched-chain fuels? Your paper provides a very nice demonstration of the influence of fuel molecular size on ignition rate. Consideration of fuel structure would be very valuable.

Author's Reply. Fuel structure is very important in determining the rate of the isomerization reaction $\dot{R}O_2 \rightleftarrows \dot{R}O_2H$ which is included in the model presented. A preliminary comparison with experiment has been made in the case of isooctane, but it was not included in the paper, partly because of space limitations, and partly because the experimental data was too uncertain to draw quantitative conclusions. Qualitative agreement was good, however.

●

C. K. Wu, Chinese Academy of Science. Would you please comment in general on the relative merits of the bomb and the rapid-compression-machine in studies of this type?

Author's Reply. There is no question that because the motion of the piston can be preprogrammed, rapid compression machines are far more versatile than constant volume bombs for basic studies of chemical reaction rates. For studies of explosion limits however, constant volume bombs have the advantages of simpler construction, lower cost, and easier operation. In addition, because the gas is compressed by a flame front, they provide a better simulation of the compression process leading to knock in firing spark-ignition engines. It is for such studies that I feel constant volume bombs are best suited and direct comparisons of explosion limits measured in constant volume bombs and rapid compression machines are essential for developing and validating reliable knock models.

●

J. Franck. In your talk you presented a diagram, an Arrhenius plot of the explosion density as a function of reciprocal temperature. Within this diagram you showed the results of some of the rapid compression work done in the 50's.

What temperature did you take when including the rapid compression data in your plot? Was it the end of compression temperature, the minimum temperature the gas experienced in the ignition delay time, or the temperature at which the gas mixture actually ignited?

At Leeds University we have found that the compression temperature might not be the right parameter since the preceeding temperature history of the gas during the delay period depends strongly on the heat loss from the gas. This also affects the ignition limit which shifts to higher temperatures as the heat loss is increased.

Could you please comment with respect to the above points on your comparison between the constant volume and the rapid compression work.

Author's Reply. The temperature used in Figure 7 to correlate explosion limits measured in the constant volume bomb and first-stage induction times measured in rapid compression machines in the 1950's was the adiabatic core gas temperature at the time a

pressure rise due to chemical reactions was first observable. This was computed from the measured pressure assuming isentropic compression of the core gas from its initial temperature and pressure. In the temperature range shown, such a correlation is justified because the second stage duration is small compared to the first stage induction time and heat losses in the rapid compression machines were negligible. A small additive correction to the induction time was necessary, however, to account for chemical reactions during compression.

Although it is true that heat loss strongly affects the mean gas temperature calculated from the Equation of State and the First Law, it does not enter the calculation of the adiabatic core gas temperature from the measured pressure. Moreover, since it is very probable that induction times and explosion limits are determined by chemical reactions in the core gas, the adiabatic core gas temperature should be a better parameter for correlating the data than the mean gas temperature which I believe was used in the analysis of the Leeds data.

In this connection, it may be noted that heat losses in the Leeds rapid compression machine (and the 1969 Thornton machine on which it is based) are much larger than those in the 1950's machines. A possible reason for this is the larger side wall vortex associated with the longer stroke of the newer machines.

●

T. Kageyama, Laboratoire d'Energetique et de Ditonigui. During similar experiments made in a spherical chamber using C_3H_8-Air mixtures, we observed such pressure rise acceleration only in the case of fuel rich mixtures with dry air? What was the state of the air utilized in your experiments and what is the applicability of your results in practical cases with humified air, such as automotive engines?

Author's Reply. The author did not provide a reply.